A Diagonal Split-cell Model for the High-order Symplectic FDTD Scheme

Wei Sha, **Xianliang Wu**, **and Mingsheng Chen**
Key Laboratory of Intelligent Computing & Signal Processing
Anhui University, Hefei 230039, China

Abstract— A high-order symplectic FDTD (SFDTD) scheme using the diagonal split-cell model is presented to analyze electromagnetic scattering of the curved three-dimensional perfectly conducting objects. One the one hand, for the undistorted cells, the fourth-order accurate spatial difference is employed. On the other hand, for the completely distorted cells, the treatment of the curved surfaces is based on the diagonal split-cell model. Finally, for the partially distorted cells, the interpolation strategy is proposed to keep the field components continuous. The numerical experiments suggest that the diagonal SFDTD scheme can obtain more accurate results than both the staircased SFDTD scheme and the traditional diagonal FDTD method. Furthermore, in view of the high numerical stability, the improved symplectic scheme does not need to decrease time increment to comply with the stability criterion.

DOI: 10.2529/PIERS060903035033

1. INTRODUCTION

As the most standard algorithm, the traditional finite-difference time-domain (FDTD) method [1], which is second-order accurate in both space and time, has been widely applied to the electromagnetic computation and simulation. Unfortunately, for electrically large domains and for long-term simulation, the method consumes large computational resources owing to the limit of numerical dispersion and stability. Up to now, some more efficient solutions have been presented. For example, in 1989, Fang proposed high-order accurate FDTD method [2], which is fourth-order accurate in both space and time. But the method is hard to treat the varying of permittivity and permeability in the inhomogeneous domain on account of the application of third-order spatial derivatives to substitute for third-order correctional temporal derivatives. Another approach is to use fourth-order accurate Runge-Kutta (R-K) method [3] in the time direction and central-difference with Yee lattice in the space direction, yet, the method is dissipative and requires additional memory.

The symplectic schemes have demonstrated their advantage in energy conservation for the Hamiltonian system over other high-order methods [4]. A symplectic FDTD (SFDTD) scheme [5–7], which is explicit fourth-order accurate in both space and time, was introduced to the computational electromagnetism by Hirono for analyzing waveguide's eigenmode. It has been verified that the SFDTD scheme is nondissipative and saves memory. Moreover, the total field and scattered field technique and the near-to-far-field transformation [8, 9] have been further developed, by which the radar cross section (RCS) of dielectric sphere was successfully computed.

However, considering the high-order difference approximation for the spatial derivatives and the staircase model for the curved surfaces, the advantage of the SFDTD scheme cannot extend to electromagnetic scattering of the curved three-dimensional perfectly conducting objects. Here the diagonal SFDTD scheme is presented to overcome the problem. The Yee cells in the scheme are classified and discriminatingly handled, which not only eliminates the spurious solutions, but also maintains the numerical results accurate.

The paper is organized as follows. The formulation of the SFDTD scheme is given in Section 2, followed by the diagonal split-cell model for treating curved surfaces specified in Section 3, numerical results are presented in Section 4, and summary is concluded in Section 5.

2. GENERAL FORMULATION

The formulation of the x component of the normalized electric field ($\widetilde{E}_x = \sqrt{\varepsilon_0/\mu_0}E_x$) for the SFDTD scheme can be written as [7]

$$\widetilde{E}_x^{n+l/m}\left(i+\frac{1}{2},\, j,\, k\right) = \widetilde{E}_x^{n+(l-1)/m}\left(i+\frac{1}{2},\, j,\, k\right) + d_l$$
$$\times\left\{\lambda_1 \times\left[CFL_y \times\left(H_z^{n+(l-1)/m}\left(i+\frac{1}{2},\, j+\frac{1}{2},\, k\right) - H_z^{n+(l-1)/m}\left(i+\frac{1}{2},\, j-\frac{1}{2},\, k\right)\right)\right.\right.$$
$$-CFL_z \times\left(H_y^{n+(l-1)/m}\left(i+\frac{1}{2},\, j,\, k+\frac{1}{2}\right) - H_y^{n+(l-1)/m}\left(i+\frac{1}{2},\, j,\, k-\frac{1}{2}\right)\right)\Big]$$
$$+\left(\frac{\lambda_2}{3}\right)\times\left[CFL_y \times\left(H_z^{n+(l-1)/m}\left(i+\frac{1}{2},\, j+\frac{3}{2},\, k\right) - H_z^{n+(l-1)/m}\left(i+\frac{1}{2},\, j-\frac{3}{2},\, k\right)\right)\right.$$
$$\left.\left.-CFL_z \times\left(H_y^{n+(l-1)/m}\left(i+\frac{1}{2},\, j,\, k+\frac{3}{2}\right) - H_y^{n+(l-1)/m}\left(i+\frac{1}{2},\, j,\, k-\frac{3}{2}\right)\right)\right]\right\} \quad (1)$$

$$CFL_y = \frac{1}{\sqrt{\mu_0\varepsilon_0}}\frac{\Delta_t}{\Delta_y} \qquad CFL_z = \frac{1}{\sqrt{\mu_0\varepsilon_0}}\frac{\Delta_t}{\Delta_z} \quad (2)$$

where Δ_y, Δ_z are, respectively, the lattice space increments in the y and z coordinate directions, Δ_t is the time increment, d_l are the constant coefficients of the symplectic integrator, i, j, k, n, l and m are integers, $n + l/m$ denotes the l-th stage after the n-th time step, and m is the total stage number. Here we use $m = 5$, a five-stage fourth-order symplectic integrator is constructed. In addition, when $\lambda_1 = 1$ and $\lambda_2 = 0$, the expression is second-order accurate in space, and when $\lambda_1 = 9/8$ and $\lambda_2 = -1/8$, that is fourth-order accurate in space.

3. DIAGONAL SPLIT-CELL MODEL

For high-order spatial difference, every H-component is surrounded by eight E-components, and vice versa. In Fig. 1(a), the near four circulating E-components equidistant to the H-component can link one closed loop referred to as L_1, and those far can link another loop L_2. The closed PEC surface is notated by S. The L_1, L_2 and S can be viewed as the point set. We treat all the cells drawn in Fig. 1(b)∼(d) according to the following strategies.

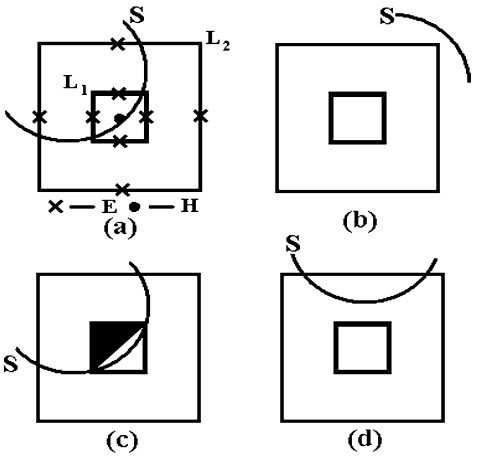

Figure 1: (a) The locations of the H-component and the E-components, (b) Undistorted cell, (c) Completely distorted cell. The black area denotes the diagonal split-cell, (d) Partially distorted cell.

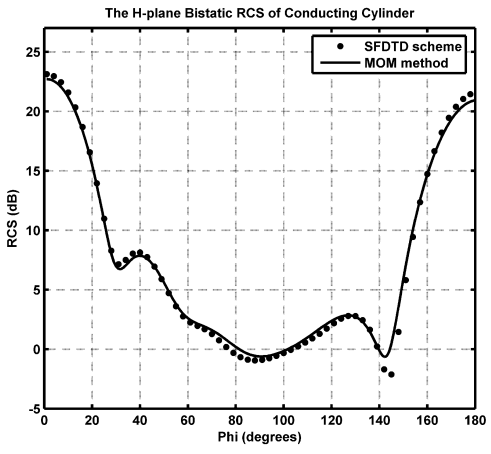

Figure 2: The bistatic RCS of conducting cylinder.

(1) Undistorted cells ($(L_1 \bigcup L_2) \bigcap S = \varnothing$). Here the fourth-order spatial difference is employed. The parameter λ_1 and λ_2 in (1) are taken to be $9/8$ and $-1/8$.

(2) Completely distorted cells ($L_1 \bigcap S \neq \varnothing$). The E-fields are treated in the traditional staircased FDTD way by setting $\lambda_1 = 1$ and $\lambda_2 = 0$. The H-fields are handled according to the diagonal split-cell model [11]. If and only if the circulating E-fields are designated as split along the cell diagonal, the H-fields are to be updated by setting $\lambda_1 = 2$ and $\lambda_2 = 0$. Besides, $\lambda_1 = 1$ and $\lambda_2 = 0$ should be set.

(3) Partially distorted cells ($L_1 \bigcap S = \varnothing$ and $L_2 \bigcap S \neq \varnothing$). Both E-fields and H-fields are initially computed by using the traditional staircased FDTD approach. Then, in order to eliminate the reflection from the undistorted cells to the completely distorted cells, the partially distorted cells are specially treated to keep the field components continuous. The interpolation equations for the E-fields and H-fields are proposed as

$$F_\delta(h) = W_1 F_\delta(h) + W_2 \times \left[\frac{1}{2}\left(F_\delta(h+1) + F_\delta(h-1)\right)\right] \tag{3}$$

$$F = \widetilde{E}, \quad H, \quad \delta = x,\, y,\, z, \quad h = i,\, j,\, k \tag{4}$$

where W_1 and W_2 are weighting coefficients satisfying $W_1 + W_2 = 1$. Generally, for $W_1 \in [0.87,\, 0.97]$, the stable and accurate numerical results can be obtained. What's more, if the incident plane wave is a unit Gaussian pulse, the largest magnitude of the field values at the partially distorted cells is below the order of 10^{-3}.

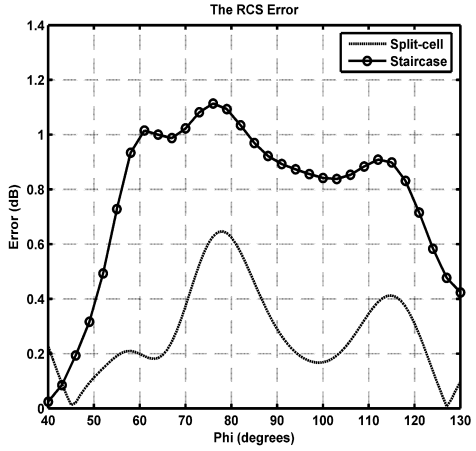

Figure 3: The absolute RCS Error.

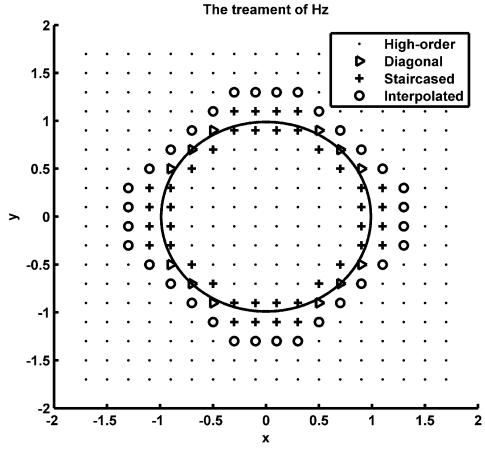

Figure 4: The location of spatial cells for the H_z component. The points denote the undistorted cells, the circles denote the partially distorted cells, and the pluses and triangles denote the completely distorted cells using the staircased and the diagonal approximation.

4. NUMERICAL RESULTS

Without loss of generality, it can be assumed that the incident plane wave with frequency of 300 MHz propagates along the z direction, and the electric field is polarized along the x direction, and the cubic grid is adopted, i.e., $\Delta_x = \Delta_y = \Delta_z = \Delta_\delta$ and $CFL_x = CFL_y = CFL_z = CFL_\delta$.

1. The scattering of conducting cylinder with the radius of 1 m and the height of 1 m is considered. The space increment and the Courant-Friedrichs-Levy (CFL) number are set to $\Delta_\delta = 0.1$ m and $CFL_\delta = 0.5$, respectively. The H-plane bistatic RCS plotted in Fig. 2 is computed by the SFDTD scheme using the diagonal split-cell model. The result calculated by the diagonal SFDTD scheme is in a good agreement with the reference solution calculated by the moment methods. The absolute RCS error curves are illustrated in Fig. 3. It can be seen that the diagonal SFDTD scheme can obtain more accurate results than the staircased SFDTD scheme. Similarly, the relative 2-norm error for the diagonal SFDTD scheme is 0.0556 compared with 0.0816 for the traditional diagonal FDTD method.

2. The monostatic RCS of conducting sphere with the radius of 1 m is calculated. The space increment is unchanged and the CFL number is retaken to $CFL_\delta = 0.70$. The Fig. 4 shows

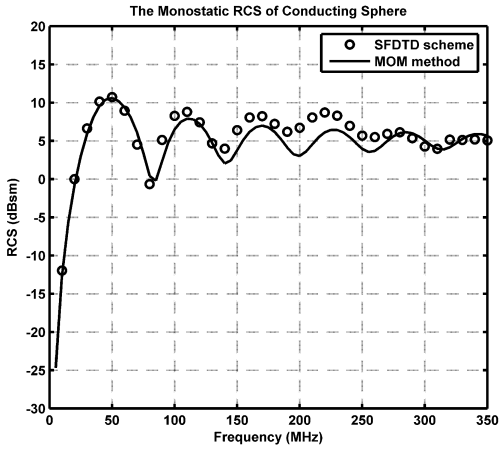

Figure 5: The monostatic RCS of conducting sphere.

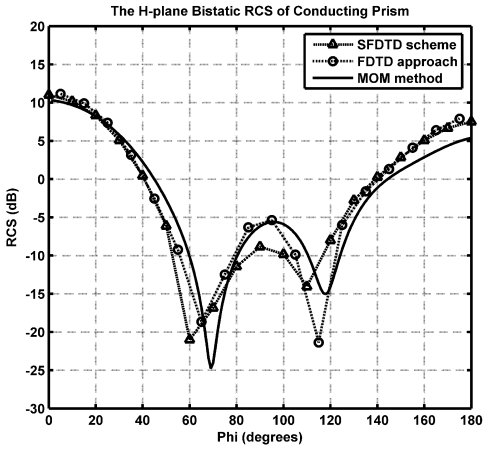

Figure 6: The bistatic RCS of conducting prism.

the location of spatial cells for the H_z component. Because of the utilization of low-order spatial difference near the curved boundaries and the symplectic structure in the time direction, the SFDTD solution shown in Fig. 5 still keeps accurate and stable after 5000 time steps.

3. The proposed scheme is employed to analyze the far response of conducting prism displayed in Fig. 6. The side length of the prism are, respectively, 1 m, 1 m, and $\sqrt{2}$ m, and the height is chosen to be 1 m. Under the same relative error condition, the diagonal SFDTD scheme occupies $71 \times 71 \times 71$ cells with $\Delta_\delta = 1.0/8.0$ and $CFL_\delta = 0.65$, by contrast, the traditional staircased FDTD approach occupies $111 \times 111 \times 111$ cells with $\Delta_\delta = 1.0/15.1$ and $CFL_\delta = 0.50$. About 32.4% memory and 39.5% CPU time are saved by the proposed scheme.

5. CONCLUSION

The high-order SFDTD scheme using the diagonal split-cell model can accurately and efficiently solve the scattering of three-dimensional perfectly conducting objects with curved metal boundaries. The high numerical stability of the scheme can obviate the instability problem due to the traditional diagonal approximation. Further more, the improved SFDTD scheme is easy to implement and places little additional computations on the original scheme. The future work will focus on the development of the proposed scheme in conjugation with the subgridding method.

ACKNOWLEDGMENT

This work was supported in part by "The national natural science foundation of China (No. 60371041)".

REFERENCES

1. Taflove, A., *Computational Electrodynamics: the Finite-Difference Time-Domain Method*, Artech House, Norwood, MA, 1995.
2. Fang, J., "Time domain finite difference computation for Maxwell's equations," *Dept. Elect. Eng.*, Ph.D. dissertation, Univ. California, Berkeley, CA, 1989.
3. Taflove, A., etc., *Advances in Computational Electrodynamics: The Finite-Difference Time-Domain Method*, Artech House, Norwood, MA, 1998.
4. Sanz-Serna, J. M. and M. P. Calvo, *Numerical Hamiltonian Problems*, Chapman & Hall, London, U.K., 1994.
5. Hirono, T., W. W. Lui, and S. Seki, "Successful applications of PML-ABC to the symplectic FDTD scheme with 4th-order accuracy in time and space," *IEEE MTT-S International Microwave Symposium Digest*, Vol. 3, 1293–1296, 1999.
6. Saitoh, I., Y. Suzuki, and N. Takahashi, "The symplectic finite difference time domain method," *IEEE Transactions on Magnetics*, Vol. 37, 3251–3254, 2001.
7. Hirono, T., W. Lui, S. Seki, and Y. Yoshikuni, "A three-dimensional fourth-order finite-difference time-domain scheme using a symplectic integrator propagator," *IEEE Transactions on Microwave Theory and Techniques*, Vol. 49, 1640–1648, 2001.

8. Zhai, P. W., G. W. Kattawar, P. Yang, and C. H. Li, "Application of the symplectic finite-difference time-domain method to light scattering by small particles," *Applied Optics*, Vol. 44, 1650–1656, 2005.
9. Sha, W., Z. X. Huang, X. L. Wu, and M. S. Chen, "Total field and scattered field technique for fourth-order symplectic finite difference time domain method," *Chinese Physics Letters*, Vol. 23, 103–105, 2006.
10. Yoshida, H., "Construction of higher order symplectic integrators," *Physica D: Nonlinear Phenomena*, Vol. 46, 262, 1990.
11. Mezzanotte, P., L. Roselli, and R. Sorrentino, "A simple way to model curved metal boundaries in fdtd algorithm avoiding staircase approximation," *IEEE Microwave and Guided Wave Letters*, Vol. 5, 267–269, 1995.